Optik - International Journal for Light and Electron Optics 274 (2023) 170526

Contents lists available at ScienceDirect

Optik

journal homepage: www.elsevier.com/locate/ijleo

Functional assessment of various rare-earth (RE) ion types: An investigation on gamma-ray attenuation properties of GeO_2-B_2O_3-P_2O_5-ZnO-Tb_2O_3-RE magneto-optical glasses

Ghada ALMisned [a], Duygu Sen Baykal [b], E. Ilik [c], Mohammed Abuzaid [d], Gokhan Kilic [c], H.O. Tekin [d,e,*]

[a] Department of Physics, College of Science, Princess Nourah Bint Abdulrahman University, P.O. Box 84428, Riyadh 11671, Saudi Arabia
[b] Istanbul Kent University, Vocational School of Health Sciences, Medical Imaging Techniques, Istanbul 34433, Turkey
[c] Eskisehir Osmangazi University, Faculty of Science and Letters, Department of Physics, TR-26040 Eskisehir, Turkey
[d] Department of Medical Diagnostic Imaging, College of Health Sciences, University of Sharjah, 27272, Sharjah, United Arab Emirates
[e] Istinye University, Faculty of Engineering and Natural Sciences, Computer Engineering Department, Istanbul 34396, Turkey

ARTICLE INFO

Keywords:
Rare-earth ions
Glasses
MCNPX
Transmission factor
Shielding

ABSTRACT

We report the functional assessment of various rare-earth (RE) ion types on gamma-ray attenuation properties of GeO_2-B_2O_3-P_2O_5-ZnO-Tb_2O_3-RE (where; RE=0; 1 %Ho, 1 %Pr, 1 %Er, 1 %Nd, 1 %Dy, 1 %Ce) magneto-optical glasses. The elemental fractions and densities of each glass sample were specified separately for the MCNPX Monte Carlo code. In addition to fundamental gamma absorption properties, Transmission Factors throughout a broad radioisotope energy range were measured. According to findings, Holmium (Ho) incorporation into the glass structure resulted in a net increase of 0.3406 g/cm^3, whereas Cerium (Ce) addition resulted in a net increase of 0.2047 g/cm^3. The Ho-doped S2 sample was found to have the greatest LAC value, despite the fact that seven glass samples exhibited identical behavior. The Ho-doped S2 sample had the lowest HVL values among the glass groups evaluated in this work, computed in the energy range of 0.015–15 MeV. The lowest EBF and EABF values were reported for Ho reinforced S2 sample with the highes LAC and density values. For all glass samples, a decrease in TF values was observed depending on the increase in thickness. Among the investigated glasses, Ho and Er reinforced samples (i.e., S2 and S4) showed the minimum TF values at used radioisotope energies. It can be concluded that Ho and Er type rare earth elements may provide the most effective gamma ray absorption properties when they are incorporated into the GeO_2-B_2O_3-P_2O_5-ZnO-Tb_2O_3 system.

1. Introduction

After William Roentgen's discovery of the X-ray in 1895, the hazards of ionizing radiation were instantly recognized. In the meanwhile, it takes till 1913 to create the technique of personal radiation protection by decreasing exposure duration, distance, and shielding. The radiation shielding guidelines were formed by recommending the use of 2-mm-thick lead shielding regardless of

* Corresponding author at: Department of Medical Diagnostic Imaging, College of Health Sciences, University of Sharjah, 27272, Sharjah, United Arab Emirates.
E-mail address: tekin765@gmail.com (H.O. Tekin).

https://doi.org/10.1016/j.ijleo.2023.170526
Received 18 November 2022; Accepted 6 January 2023
Available online 7 January 2023

generator voltage, filtration, or workload [1]. According to the standard for shielding while using radium, tubes and applicators should contain at least 5 cm of lead for every 100 mg of radium. The lead-based shield is an efficient shielding material with considerable drawbacks, including high toxicity, limited chemical stability, and poor flexibility [2–4]. As a consequence of the disadvantage, scientists make effort to develop significant and efficient radiation shielding materials. Glass is the contemporary shielding material against numerous forms of radiation in medical and nuclear applications. The mechanical, chemical, and optical characteristics of the reinforced glasses provide protection against gamma, neutron, and x-ray radiation. In radiology and medical imaging, it is essential to see patients during exposure; glass shields are regarded as indispensable. Lead glass is also used as box containers and hot cells for the storage of radioactive substances. Glass should have been combined with heavy metal oxides (HMO) such as lead oxide (PbO) and bismuth oxide (Bi_2O_3) for use in radiation shielding [5]. The new composite offered glass the same radiation-absorption capabilities as concrete with visibility qualities. Although lead is often used and effective, it reduces the hardness and melting point of glass. Environmental issues surrounding the use of lead have prompted research on other forms of HMO glass for radiation shielding. This includes silicon, barium, tellurium, and rare-earth element oxides. Due to their unique properties, heavy metal oxide-doped glasses have garnered considerable scientific interest. Due to these properties, the glasses are useful in a variety of technical fields. Due to their enormous energy gaps, high refractive index, and high polarizability, some glass materials have found use in thermal tensors, electrical, and optical systems [6]. There are several uses for rare-earth elements, including lasers, glass, electrical and industrial operations. In the periodic table, rare earth includes the Lanthanide family of Fifteen elements, including Yttrium. Chemically, rare earth is known a powerful limiting reagent [7]. Commonly, these compounds have high melting and boiling temperatures and are ionic. Rare earths are often softer in their metallic state than elements with higher atomic numbers. Therefore, interactions between rare earths and other metallic and nonmetallic elements result in the formation of compounds with diverse chemical characteristics. The radiation absorption characteristics of different types of glasses containing rare earth ions, on the other hand, attracted the attention of researchers and motivated the presentation of many significant reports on this subject. In a previous study, Vani et al. [8] investigated the radiation absorption improvements provided by adding some rare earth ions to barium tellurite glasses. Based on their findings, thulium-doped glasses exhibited the maximum linear attenuation coefficient at 0.245 MeV and 1.18 cm^{-1}, followed by erbium-doped glasses, holmium-doped glasses, and the base barium tellurite glass under study. Nevertheless, half-value layers and mean free routes followed the opposite pattern, with the lowest value for 2 mol. % Thulium, indicating that thulium-doped samples are superior. According to the literature [9–12], barium tellurite glasses with a greater concentration of thulium dopants have showed promise as high-energy radiation shielding materials. In another study, Alharshan et al., [13] have investigated some bismuth silicate glasses doped with the rare-earth oxides-CeO_2/Nd_2O_3/Sm_2O_3/Eu_2O_3. Their results showed that rare-earth ion doped BS-X glasses shown more effective shielding capacity than conventional photon shields such concrete, commercial-glasses, and newly explored heavy glasses, polymer, and some rocks. Numerous investigations in the literature have shown that the optical characteristics of glass structures made by doping rare-earth (RE) elements alter dramatically [14–18]. It is clear that the density of the base glass structure can be increased as a result of the addition of rare-earth elements such as Ce, Dy, Nd, Er, Pr, and Ho to the glass compositions discussed in this study. This was attributed to the fact that the glass structure interval may permit large-radius RE ions, hence increasing glass density [19]. Based on the findings of previous research [20], the corrosion resistance of the glass network structures will be larger the stronger the link between the network structures. As their chemical properties are similar to those of alkali metal oxides and alkaline earth metal oxides, rare earth oxides are used to enhance the network. Incorporating a RE oxide into the glass composition has also been proven to result in a non-bridging oxygen number. According to XRD analyses of glasses doped with rare-earth elements, these novel forms of amorphous glasses distant from crystallinity may be created [19]. The aim of this study was to closely examine the changes that occur according to the rare-earth ion type by investigating the radiation absorption properties of some paramagnetic magneto-optical glasses, which are doped with different types of rare-earth ions.

2. Materials and methods

2.1. Investigated glass strauctur̈e

In this work, Zhou and Zhu's [19] base magneto-optical glasses doped with different types of rare-earth (RE) elements such as Holmium (Ho), Praseodymium (Pr), Erbium (Er), Neodymium (Nd), Dysprosium (Dy), and Cerium (Ce) were extensively studied. The melt-quenching method provided glasses with the following basic glass compositions: 32GeO_2-15B_2O_3-5 P_2O_5-3ZnO-45Tb_2O_3-RE (RE=0; 1 %Ho, 1 %Pr, 1 %Er, 1 %Nd, 1 %Dy, 1 %Ce). The melting temperature for each glass is 1500 °C and the melting time is 60 min. After this process, the annealing temperature was 600 °C and the annealing time was 120 min. Here, base glass doped with various RE ions was combined with the glass network former (germanium borate) and network modifier ZnO, and P_2O_5. Detailed information can be obtained from the reference study where magneto-optical properties are examined [19].

2.2. Monte Carlo simulations and computational phase for shielding parameters

In this study, the gamma ray absorption properties and transmission factors of several glasses doped with rare earth ions were examined. The gamma-ray transmission factor (TF) is defined as the ratio of the number of primary gamma rays incident on an absorbing material to the number of gamma rays remaining after interaction with the absorbing material [21]. Knowing this value also provides the proportion of gamma rays absorbed by the absorber material by quantitatively measuring the absorption characteristics of a certain material. In this work, Monte Carlo code MCNPX (*version 2.7.0*) [22]was used to calculate TF values. By constructing simulation input code, all required inputs were defined prior to the simulation. As seen in Fig. 1a, two circular detection regions were

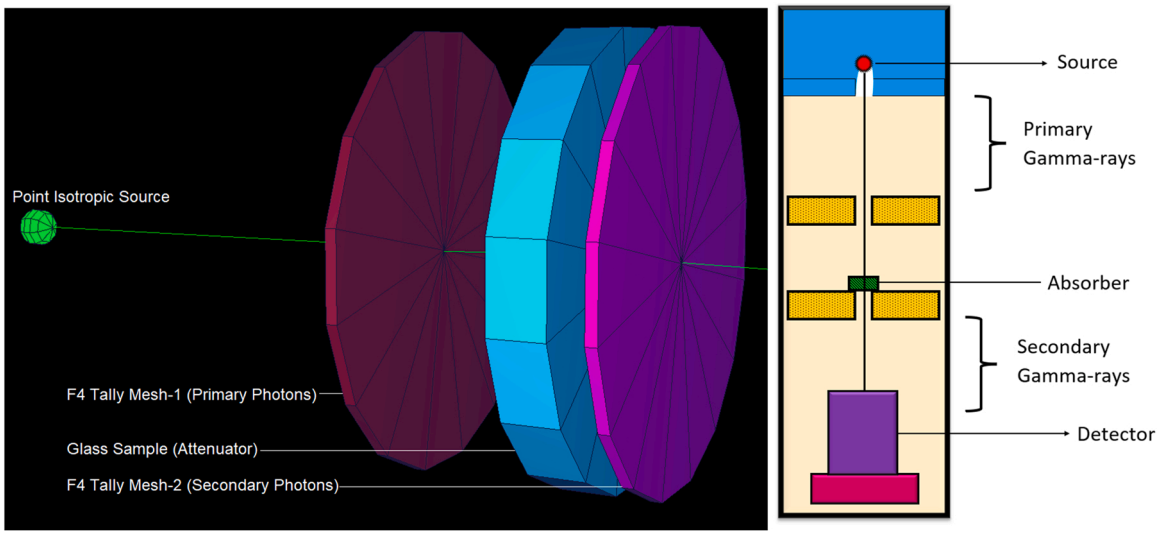

Fig. 1. (a) 3-D view of Gamma-ray transmission setup obtained from MCNPX Visual Editor (b) A general-view of gamma-ray attenuation process through an attenuator sample.

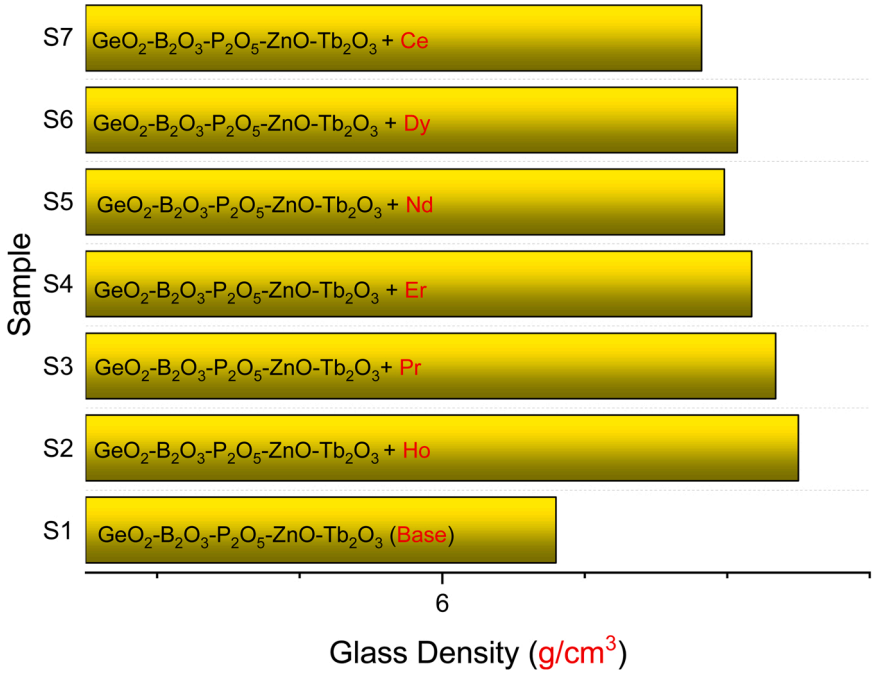

Fig. 2. Variation of glass densities from S1 to S7.

formed in the continuation of the point radioactive source and beyond the absorber glass material. Utilizing F4 Tally Mesh, the quantification of gamma rays traveling through the circular detection zones was measured. The information provided by the F4 tally mesh in the MCNPX code is the average photon flux that passes through a specific volume or point. In our research, the gamma ray flux from the source was measured in the yellow detection zone, while the secondary gamma ray flux was recorded in the purple detection zone. The ratios of the acquired values were then calculated. In the center of the two detection zones, the glass material in which the absorption process occurs is defined. Simulations were performed many times for each radioisotope energy and seven different glass materials. The simulations were conducted with 10^8 cycles (NPS) and no energy cut-off value was specified. In the input file, the radiation type that the code will track is specified as photons and neutrons are excluded. This approach is considered a variance reduction technique for MCNPX and many Monte Carlo simulation codes, and it is a crucial technique for improving simulation efficiency and lowering error rates. Next, various gamma-ray attenuation parameters of the examined glasses were calculated through

Table 1
Sample codes, composition, elemental weight fractions and densities of GeO_2-B_2O_3-P_2O_5-ZnO-Tb_2O_3-RE (where; RE=0; 1 %Ho, 1 %Pr, 1 %Er, 1 %Nd, 1 %Dy, 1 %Ce).

Sample code	B	O	P	Zn	Ge	Tb	RE (X)	Density (g/cm^3)
S1	0.046586	0.294414	0.021821	0.024103	0.222115	0.390961	-	6.1613
S2	0.046124	0.292757	0.021605	0.023864	0.219916	0.38709	**X = Ho** 0.008643	6.5019
S3	0.046124	0.293205	0.021605	0.023864	0.219916	0.38709	**X = Pr** 0.008195	6.4697
S4	0.046124	0.292741	0.021605	0.023864	0.219916	0.38709	**X = Er** 0.008659	6.436
S5	0.046124	0.292911	0.021605	0.023864	0.219916	0.38709	**X = Nd** 0.008489	6.3977
S6	0.046124	0.292773	0.021605	0.023864	0.219916	0.38709	**X = Dy** 0.008627	6.4159
S7	0.046124	0.29334	0.021605	0.023864	0.219916	0.38709	**X = Ce** 0.00806	6.366

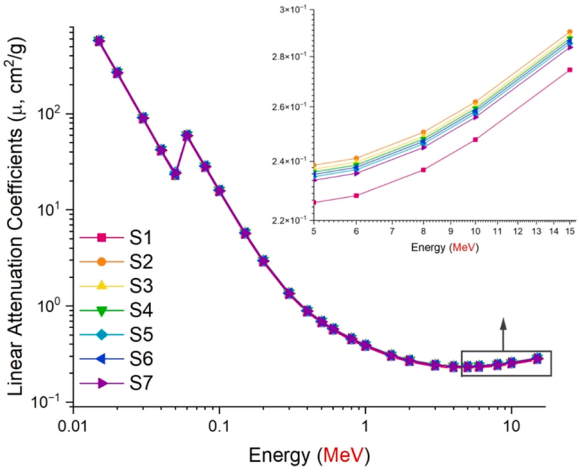

Fig. 3. : Variations of linear attenuation coefficients (cm^{-1}) as a function of photon energy (MeV) for S1-S7 glasses.

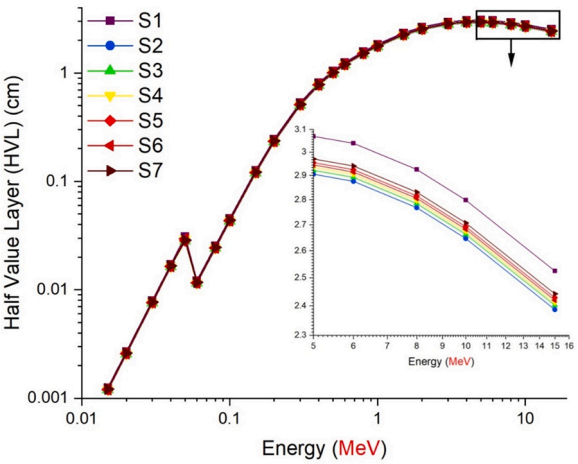

Fig. 4. Variations of half value layer (cm) as a function of photon energy (MeV).

the Phy-X/PSD [23] program. Various characteristics may be calculated to determine the gamma-ray absorption qualities of a material. In the wider definition, the attenuation coefficients of the absorbent material are provided by the transmission configuration shown in Fig. 1b. The data produced from such an arrangement enable the assessment and quantification of the material's reduction characteristics.

3. Results and discussions

In this work, the functional properties of various types of rare-earth elements, such as Ho, Pr, Er, Nd, Dy, and Ce, which are

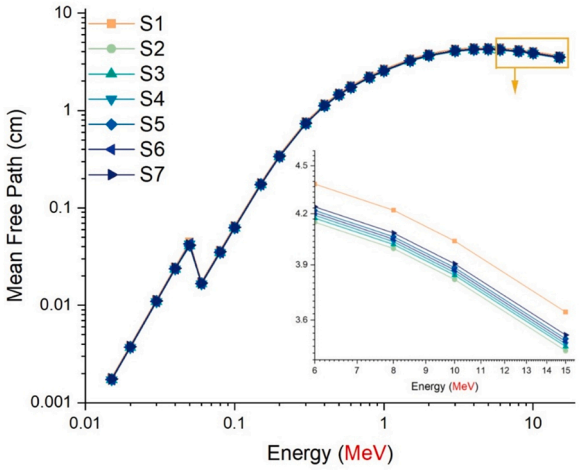

Fig. 5. Variations of mean free path (cm) values as a function of photon energy (MeV) for S1-S7 glasses.

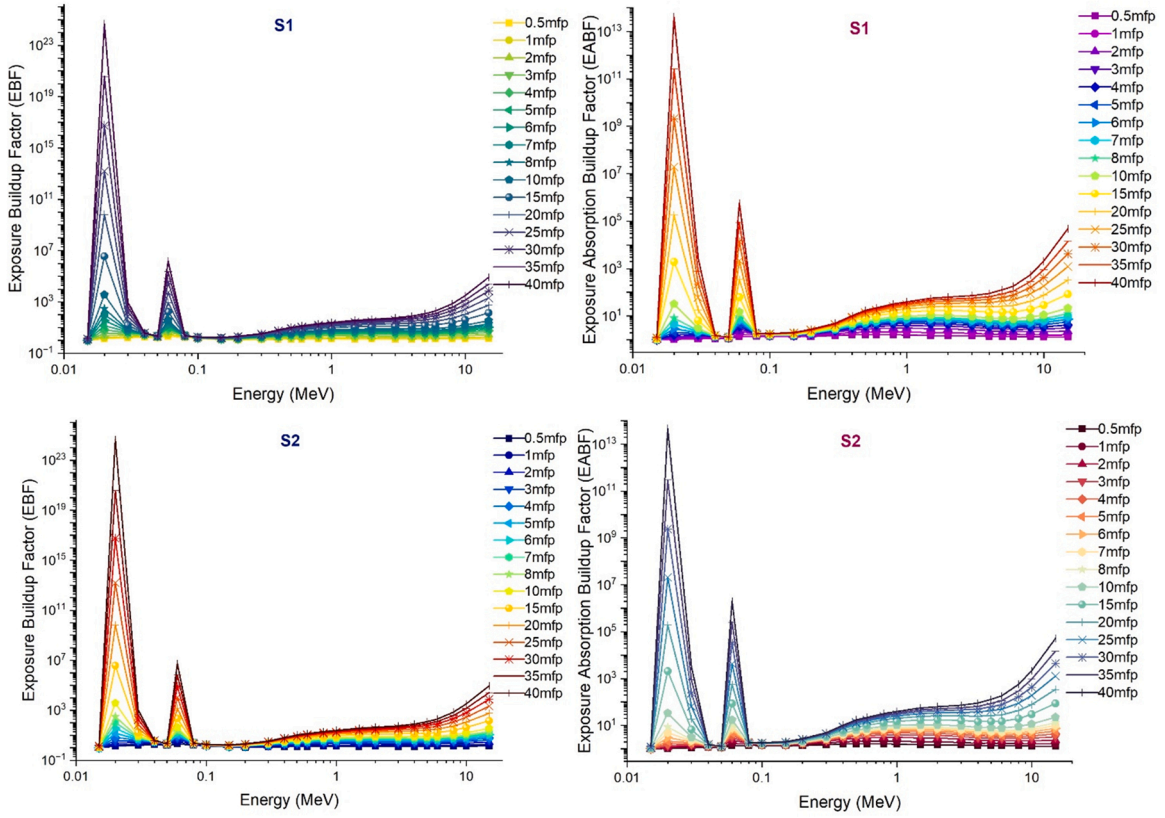

Fig. 6. Variation of exposure buildup factors (EBF) and energy absorption buildup factor (EABF) of investigated glasses at different mean free path values (from 0.5 mfp to 40 mfp).

introduced individually to the GeO_2-B_2O_3-P_2O_5-ZnO-Tb_2O_3 glass system were explored in depth and the gamma-ray attenuation properties parameters were assessed using advanced Monte Carlo simulation methods and computational tools. The linear attenuation coefficient (LAC, μ) is a density-dependent parameter measured in cm^{-1} [24,25]. Fig. 2 depicts the change in glass density as a function of the rare earth element type added. The base glass composition (S1) without rare earth element solids (i.e. GeO_2--B_2O_3-P_2O_5-ZnO-TbO_3) has the lowest glass density of 6.1613 g/cm^3, as seen in the figure. In addition to the doping, as a consequence of the transition from S2 to S7 glass composition, the glass densities have also changed. As seen in Table 1, the addition of Holmium (Ho)

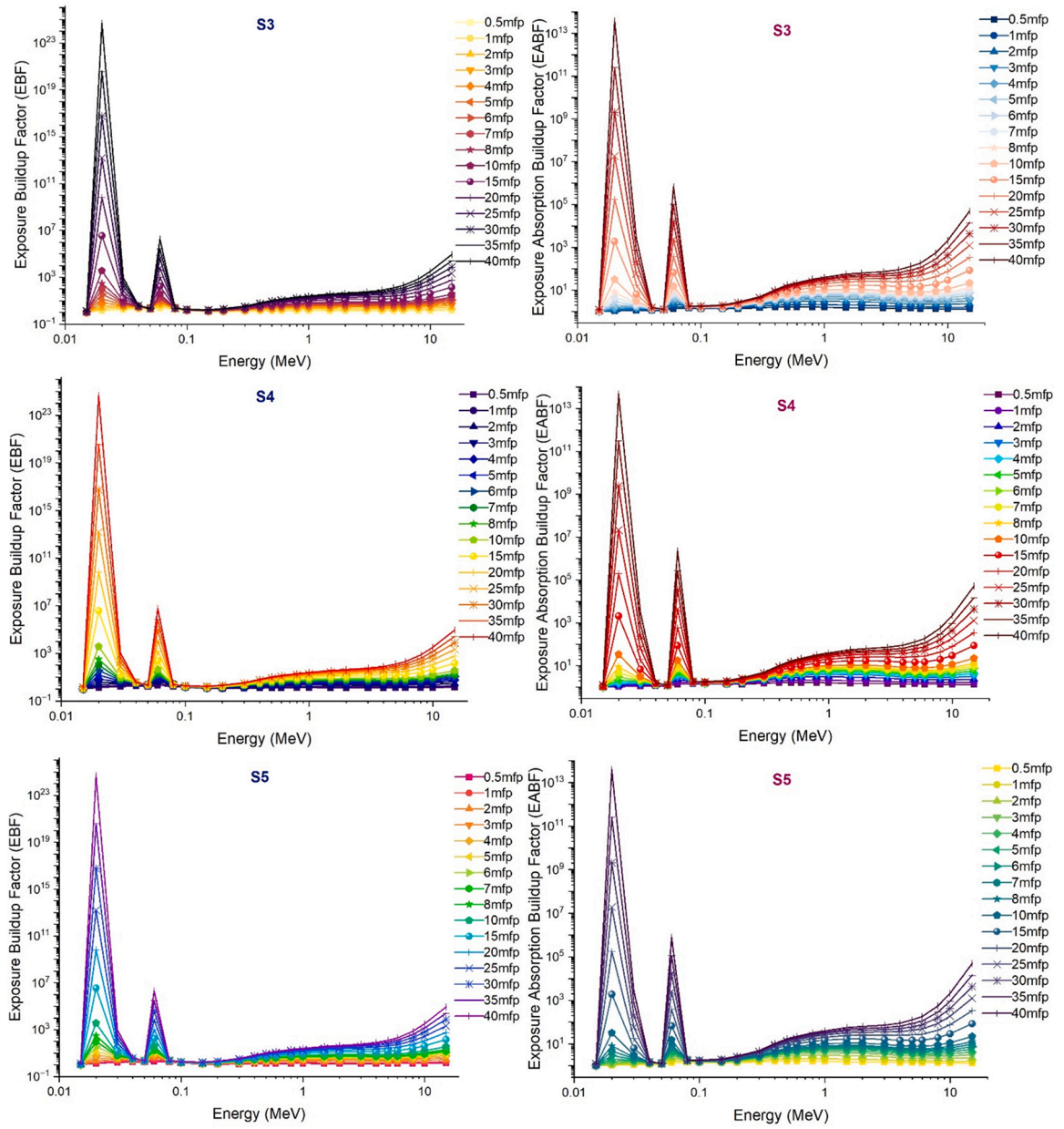

Fig. 6. (*continued*).

to the base glass composition caused the greatest increase in density, whereas Cerium (Ce) caused the least increase. Ho adding resulted in a net increase of 0.3406 g/cm^3, whereas Cerium (Ce) addition resulted in a net increase of 0.2047 g/cm^3. This may be explained by the difference between Ho's (Z_{Ho} =67) and Ce's (Z_{Ce} =57) atomic numbers and the indirect influence of this difference on the glass density. Fig. 3 depicts the variation of LAC values obtained from a GeO_2-B_2O_3-P_2O_5-ZnO-TbO_3 glass system with doped earth elements as a function of photon energy. As seen in the figure, LAC values in the low energy region have attained their maximum quantitative values. The available energy values in this region are those that cause the photoelectric effect to predominate during the photon-matter interaction, and this region is known as the low energy region [26,27]. Here, the low-energy photons on the absorber material interact with the electrons in the material medium's orbit, donating all of their energy to this interaction and undergoing total absorption. With a rise in photon energy, electrons in this orbit are ejected, and photons with decreasing energy are released to create secondary and subsequent interactions. In this situation, Compton Scattering is the predominant photon-matter interaction type in the mid-energy zone. According to Fig. 3, LAC values declined in the mid-energy zone and reached their minimum in the high-energy region (where the dominant interaction type is pair production). The Ho-doped S2 sample was found to have the greatest LAC value, despite the fact that seven glass samples exhibited identical behavior. The close proximity of LAC values in the energy range of

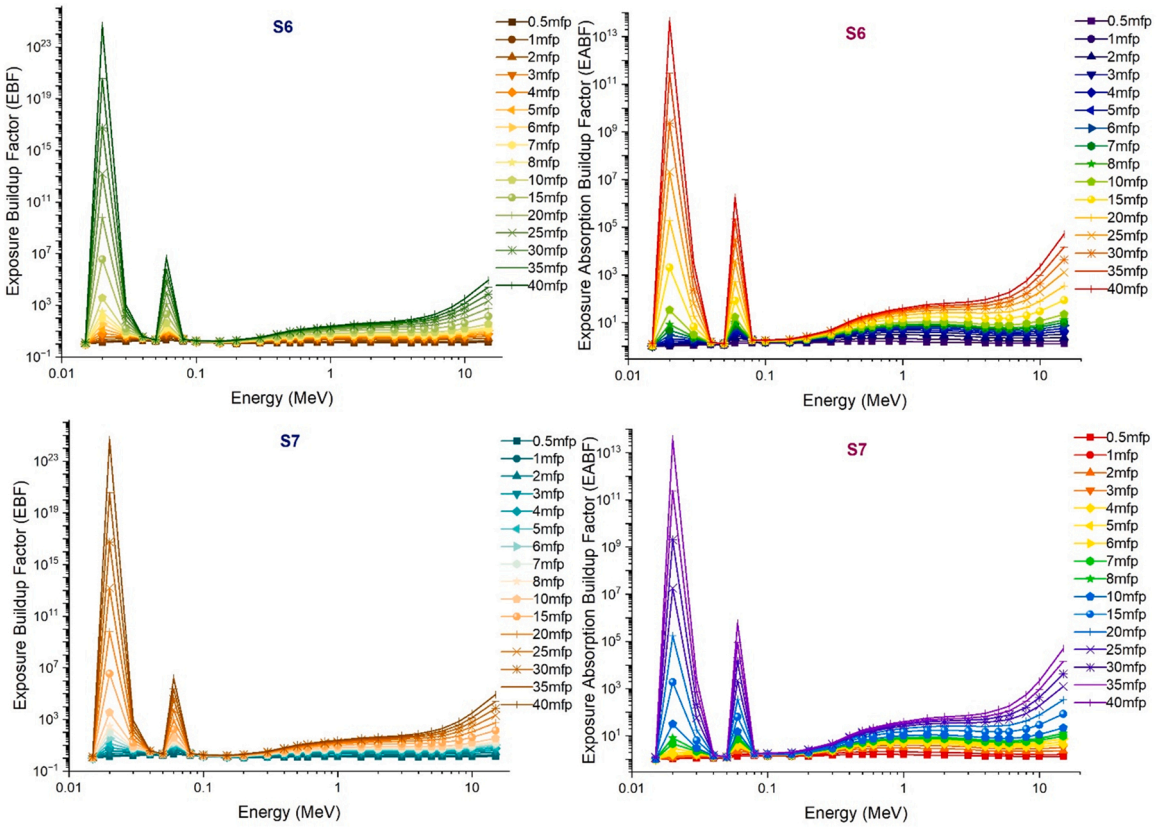

Fig. 6. (*continued*).

0.015–15 MeV is due to the low amount of rare earth element translocation and the negligible effect of this lowness on the glass density. HVL, which is computed using the LAC value, plays a crucial role in calculating the material thickness in cm that halves the photon quantity at a given energy [28]. Due to the good absorption properties of a shielding material, this value would have low values for a given energy value, indicating that the abovementioned halving process occurs at thinner material thicknesses [29]. Fig. 4 illustrates the variation of HVL values as a function of energy. As seen in the figure, although all glasses in the low-energy region have minimal HVL values, HVL values also tend to grow with an increase in energy value and vary from minimum to maximum values. In other words, the lowest HVL values for low energy regions and the maximum HVL values for high energy regions are regarded as quantitatively responsible values. This phenomenon may be explained by the relationship between penetration characteristics and gamma energy, which demonstrates that even in very thin materials, low-energy gamma rays are quantitatively absorbed. For the halving of gammas with high energy and consequently great penetrating qualities, however, the material thickness must be increased. The Ho-doped S2 sample had the lowest HVL values among the glass groups evaluated in this work, computed in the energy range of 0.015–15 MeV. This indicates that a gamma ray beam with the same energy value may be halved using S2 samples with smaller thicknesses. This situation is likewise connected to S2's maximum LAC values. The following formula expresses the minimal HVL values that would be generated by the maximum LAC values, and the inverse ratio between them is the mathematical explanation for this situation [30].

$$HVL = \ln(2) / \mu \quad (1)$$

Fig. 5 illustrates the variations that occur in the mean free path as a function of the energy of the incoming photon for glasses S1 through S5. This graph shows that the type of rare earth element has an influence on the carachteristics of mean free path values. As it is seen from the Fig. 5 that S2 sample has the minimum mfp values valies. The lower mfp values may be regarded to the better gamma-ray attenuation properties of the shielding materials. This is due to the fact that a decrease in the value of the mean free path indicates a decrease in the distance between two subsequent gamma ray interactions in the material [31]. This suggests that the absorption process may be more effective at shorter distances. As a result, the values are at their minimum for the S2 glass sample when the photon energy is 15 MeV, while they are at their greatest for the S1 glass sample. The gamma-ray energy (MeV) dependence of changes in the exposure build-up factor (EBF) and the energy absorption build-up factor (EABF) throughout a range of mean free path values is shown in Fig. 6, respectively. Because photoelectric absorption is responsible for the large majority of incoming gamma rays, the EBF and EABF values are both relatively low in the low gamma-ray energy range. According to the findings that we obtained, when the Ho was incorporated into the GeO_2-B_2O_3-P_2O_5-ZnO-Tb_2O_3 system, both the EBF and EABF values went down (i.e., from 0.5 to 40 mfp). The

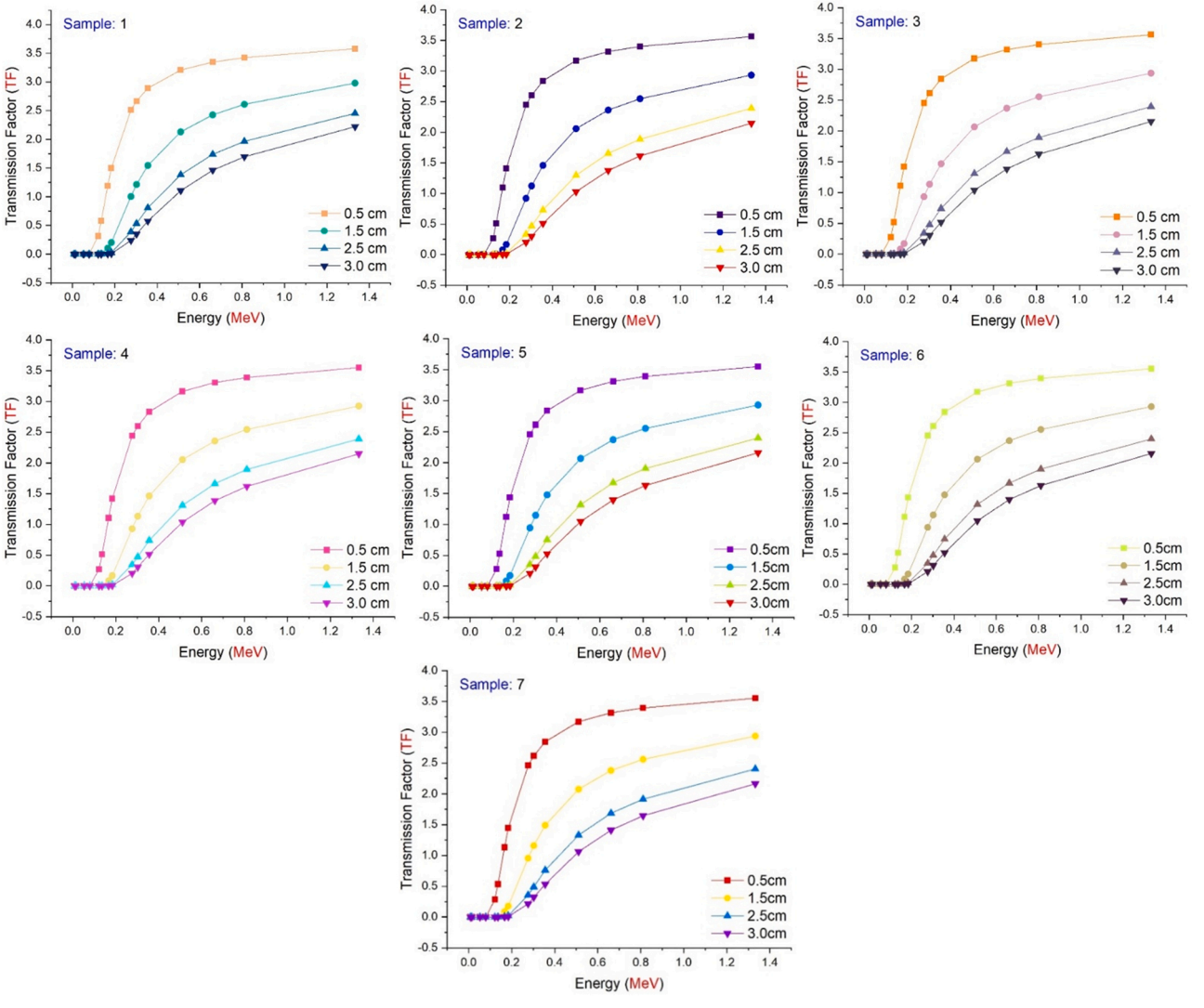

Fig. 7. Transmission Factors (TFs) of investigated glasses as a function of used radioisotope energy (MeV) at different glass thicknesses.

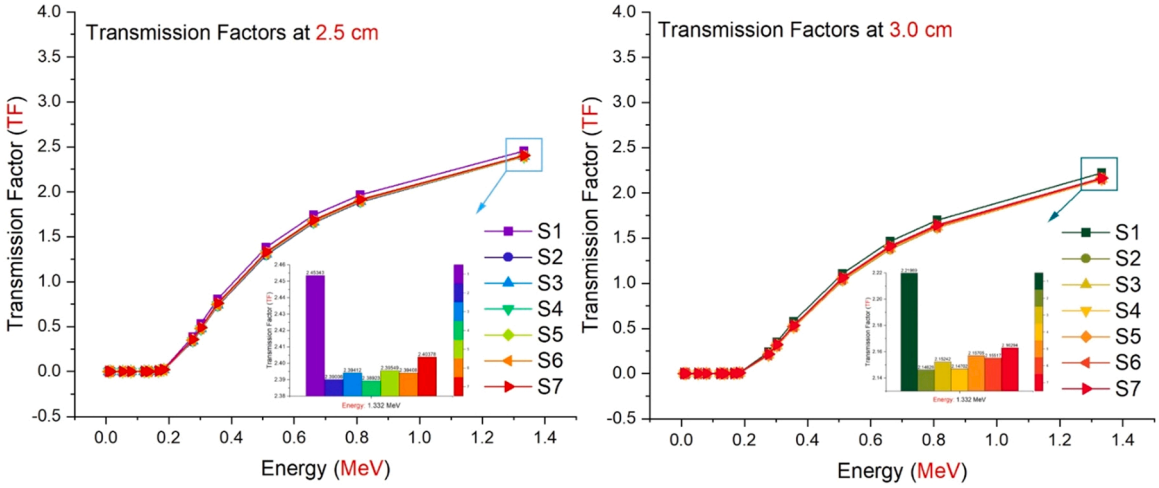

Fig. 8. Comparison of the Transmission Factors (TFs) as a function of used radioisotope energy (MeV) for different glass thicknesses.

lowest EBF and EABF values were reported for Ho reinforced S2 sample with the highes LAC and density values. The gamma-ray transmission factor (TF), which is an essential metric for shielding materials, was calculated for S1, S2, S3, S4, S5, S6 and, S7 samples over a range of well-known radioisotope energies. This range includes the following radioisotopes: ^{67}Ga (0.0086, 0.0093, 0.1840 MeV), ^{57}Co (0.0144, 0.1221, 0.1365 MeV), ^{111}In (0.0230, 0.1710, ^{60}Co (1.1732, 1.3325 MeV). Two distinct approaches were used in the analysis to determine the TF values of the glasses. In the beginning, glass thicknesses were used in order to do an analysis on the TF factors of samples S1 through S7. Fig. 7 depicts the transmission factors (TFs) of investigated glasses as a function of used radioisotope energy (MeV) at different glass thicknesses. The transmission factor changes from 0.0086 MeV to 1.3325 MeV as the energy of the radioisotope increases. Glass samples evaluated at low energies had the lowest TF values for all observed thicknesses. Due to their great attenuation capacity, thicker samples may have an easier time attenuating low-energy gamma rays. Consequently, there is a discrepancy of around 0.1 MeV. At energies larger than 0.1 MeV, glass samples become more reactive. All 3-centimeter-thick glass samples had their maximum attenuation determined (i.e., minimum transmission). Increases in shield thickness decrease gamma-ray attenuation because shield thickness impacts the efficiency of any shielding material. The TF values of the glasses were then meticulously evaluated by taking into account the attenuation capacities of different glass thicknesses. For all glass samples, a decrease in TF values was observed depending on the increase in thickness. This is due to the observation of secondary, that is, reduced gamma-ray quantity, in thicker materials. Meanwhile, Fig. 8 illustrates TFs as a function of radioisotope energy (MeV) utilized for various glass thicknesses. As shown in Fig. 8, Ho and Er reinforced samples (S2 and S4) had the lowest TF values at the radioisotope energies used. From these results, it can be concluded that Ho and Er type rare earth elements may provide the most effective gamma ray absorption properties when they are incorporated into the GeO_2-B_2O_3-P_2O_5-ZnO-Tb_2O_3 system.

4. Conclusions

This research looked on rare earth element oxide doped glass series with amorphous qualities. Six rare earth elements, which have a regulatory effect on their structural properties, were selected and the performances of previously synthesized glass structures against radiation effects were evaluated. The relatively large densities of rare earth element oxides, as is well known, can contribute to the physical characteristics of the fabricated glasses such as density. One of the most essential aspects of radiation shielding research is related material's density change. For the very reason, the preference in this study was for rare earth elements, which have a density-increasing impact. The following conclusion have been provided to the scientific community in light of the study's findings.

- The base glass composition (S1) without rare earth element solids (i.e. GeO_2-B_2O_3-P_2O_5-ZnO-TbO_3) has the lowest glass density of 6.1613 g/cm^3.
- Ho incorporation into the glass structure resulted in a net increase of 0.3406 g/cm^3, whereas Cerium (Ce) addition resulted in a net increase of 0.2047 g/cm^3.
- The Ho-doped S2 sample was found to have the greatest LAC value, despite the fact that seven glass samples exhibited identical behavior.
- The Ho-doped S2 sample had the lowest HVL values among the glass groups evaluated in this work, computed in the energy range of 0.015–15 MeV.
- The lowest EBF and EABF values were reported for Ho reinforced S2 sample with the highes LAC and density values.
- For all glass samples, a decrease in TF values was observed depending on the increase in thickness.
- Ho and Er reinforced samples (i.e., S2 and S4) showed the minimum TF values at used radioisotope energies.

It can be concluded that Ho and Er type rare earth elements may provide the most effective gamma ray absorption properties when they are incorporated into the GeO_2-B_2O_3-P_2O_5-ZnO-Tb_2O_3 system.

Declaration of Competing Interest

None.

Data Availability

Data will be made available on request.

Acknowledgement

The authors would like to express their deepest gratitude to Princess Nourah bint Abdulrahman University Researchers Supporting Project number (PNURSP2023R149), Princess Nourah bint Abdulrahman University, Riyadh, Saudi Arabia.

References

[1] J.K. Shultis, R.E. Faw, Radiation shielding technology, Health Phys. 88 (4) (2005) 297–322, https://doi.org/10.1097/01.HP.0000148615.73825.b1.
[2] M.A. Alothman, A.M. Al-Baradi, S.B. Ahmed, R. Kurtulus, I.O. Olarinoye, T. Kavas, M.S. Al-Buriahi, Physical, optical, and ionizing radiation shielding parameters of Al (PO3) 3-doped PbO–Bi2O3–B2O3 glass system, J. Mater. Sci.: Mater. Electron. 32 (23) (2021) 27744–27761, https://doi.org/10.1007/s10854-021-07157-x.
[3] F. Laariedh, M.I. Sayyed, A. Kumar, H.O. Tekin, R. Kaur, T.B. Badeche, Studies on the structural, optical and radiation shielding properties of (50–x) PbO–10 WO3–10 Na2O–10 MgO–(20+ x) B2O3 glasses, J. Non-Cryst. Solids 513 (2019) 159–166, https://doi.org/10.1016/j.jnoncrysol.2019.03.007.
[4] S.A. Issa, L.R.P. Kassab, G. Susoy, M.V.M. Nishimura, G.R. da Silva Mattos, C.D.S. Bordon, H.O. Tekin, Fabrication, optical characteristic, and nuclear radiation shielding properties of newly synthesised PbO–GeO2 glasses, Appl. Phys. A 126 (9) (2020) 1–15, https://doi.org/10.1007/s00339-020-03928-1.
[5] K. Kirdsiri, J. Kaewkhao, N. Chanthima, P. Limsuwan, Comparative study of silicate glasses containing Bi2O3, PbO and BaO: Radiation shielding and optical properties, Ann. Nucl. Energy 38 (6) (2011) 1438–1441, https://doi.org/10.1016/j.anucene.2011.01.031.
[6] A. Alhodaib, O. Ibrahim, S. Abd El All, F. Ezzeldin, Effect of rare-earth ions on the optical and pl properties of novel borosilicate glass developed from agricultural waste, Materials (Basel) 14 (19) (2021) 5607, https://doi.org/10.3390/ma14195607.
[7] S. Gai, C. Li, P. Yang, J. Lin, Recent progress in rare earth micro/nanocrystals: soft chemical synthesis, luminescent properties, and biomedical applications, Chem. Rev. 114 (4) (2014) 2343–2389, https://doi.org/10.1021/cr4001594.
[8] P. Vani, G. Vinitha, M.I. Sayyed, Maha M. AlShammari, N. Manikandan, Effect of rare earth dopants on the radiation shielding properties of barium tellurite glasses, Nucl. Eng. Technol. 53 (12) (2021) 4106–4113, https://doi.org/10.1016/j.net.2021.06.009.
[9] K. Boonin, P. Yasaka, P. Limkitjaroenporn, R. Rajaramakrishna, A. Askin, M.I. Sayyed, S. Kothan, J. Kaewkhao, Effect of BaO on lead free zinc barium tellurite glass for radiation shielding materials in nuclear application, J. Non-Cryst. Solids 550 (2020), 120386, https://doi.org/10.1016/j.jnoncrysol.2020.120386.
[10] P. Vani, G. Vinitha, M.I. Sayyed, M.M. AlShammari, N. Manikandan, Effect of rare earth dopants on the radiation shielding properties of barium tellurite glasses, Nucl. Eng. Technol. 53 (12) (2021) 4106–4113, https://doi.org/10.1016/j.net.2021.06.009.
[11] M.I. Sayyed, B.O. El-bashir, A.M. Alhuthali, Y.S.M. Alajerami, Y. Al-Hadeethi, M.H.A. Mhareb, Gamma radiation shielding and structural features for barium strontium boro-tellurite glass modified with various concentrations of molybdenum oxide, J. Non-Cryst. Solids 559 (2021), 120658, https://doi.org/10.1016/j.jnoncrysol.2021.120658.
[12] K.A. Naseer, K. Marimuthu, M.S. Al-Buriahi, A. Alalawi, H.O. Tekin, Influence of Bi2O3 concentration on barium-telluro-borate glasses: physical, structural and radiation-shielding properties, Ceram. Int. 47 (1) (2021) 329–340, https://doi.org/10.1016/j.ceramint.2020.08.138.
[13] Gharam A. Alharshan, Canel Eke, Z.A. Alrowaili, Samia ben Ahmed, I.O. Olarinoye, M.S. Al-Buriahi, Influence of rare-earth ions on the radiation protection ability of some optical glasses containing Bi2O3 and SiO2, Optik 264 (2022), 169371, https://doi.org/10.1016/j.ijleo.2022.169371.
[14] G. ALMisned, H.O. Tekin, A. Ene, S.A. Issa, G. Kilic, H.M. Zakaly, A closer look on nuclear radiation shielding properties of Eu3+ doped heavy metal oxide glasses: impact of Al2O3/PbO substitution, Materials 14 (18) (2021) 5334, https://doi.org/10.3390/ma14185334.
[15] S. Tanabe, Optical transitions of rare earth ions for amplifiers: how the local structure works in glass, J. Non-Cryst. Solids 259 (1-3) (1999) 1–9, https://doi.org/10.1016/S0022-3093(99)00490-1.
[16] Y. Shen, Y. Lu, X. Yu, Z. Liu, Effect of temperature on characteristics of rare earth-doped magneto-optical glass in optical current transducer application, Optik 126 (23) (2015) 3589–3593, https://doi.org/10.1016/j.ijleo.2015.08.249.
[17] G. Kilic, E. Ilik, S.A. Issa, H.O. Tekin, Synthesis and structural, optical, physical properties of Gadolinium (III) oxide reinforced TeO2–B2O3–(20-x) Li2O-xGd2O3 glass system, J. Alloy. Compd. 877 (2021), 160302, https://doi.org/10.1016/j.jallcom.2021.160302.
[18] L. Feng, L. Bian, J. Nie, H. He, C. Liu, Optical properties and upconversion in rare earth doped oxyfluoride glasses, Optik 169 (2018) 118–124, https://doi.org/10.1016/j.ijleo.2018.05.042.
[19] L. Zhou, Z. Zhu, Study of magneto-optical properties of GeO2-B2O3-P2O5-ZnO-Tb2O3 glass doped with different rare-earth ions, J. Non-Cryst. Solids 576 (2022), 121241, https://doi.org/10.1016/j.jnoncrysol.2021.121241.
[20] X. Gao, Q. Zhang, J. Yu, W. Tang, Y. Li, A. Lu, Effect of replacement of Al2O3 by Y2O3 on the structure and properties of alkali-free boro-aluminosilicate glass, J. Non-Cryst. Solids 481 (2018) 98–102, https://doi.org/10.1016/j.jnoncrysol.2017.10.032.
[21] R. Biswas, H. Sahadath, A.S. Mollah, M.F. Huq, Calculation of gamma-ray attenuation parameters for locally developed shielding material: polyboron, J. Radiat. Res. Appl. Sci. 9 (1) (2016) 26–34, https://doi.org/10.1016/j.jrras.2015.08.005.
[22] RSICC Computer Code Collection, MCNPX User's Manual Version 2.4.0. Monte Carlo N-Particle Transport Code System for Multiple and High Energy Applications; 2002.
[23] E. Şakar, Ö.F. Özpolat, B. Alım, M.I. Sayyed, M. Kurudirek, Phy-X/PSD: development of a user friendly online software for calculation of parameters relevant to radiation shielding and dosimetry, Radiat. Phys. Chem. 166 (2020), 108496, https://doi.org/10.1016/j.radphyschem.2019.108496.
[24] M.I. Sayyed, H.O. Tekin, Malaa M. Taki, M.H.A. Mhareb, O. Agar, E. Sakar, M. Kawa, Kaky, Bi_2O_3-B_2O_3-ZnO-BaO-Li_2O glass system for gamma ray shielding applications, Optik 201 (2020), 163525, https://doi.org/10.1016/j.ijleo.2019.163525.
[25] M.I. Sayyed, H.O. Tekin, Malaa M. Taki, M.H.A. Mhareb, O. Agar, E. Sakar, M. Kawa, Kaky, Bi_2O_3-B_2O_3-ZnO-BaO-Li_2O glass system for gamma ray shielding applications, Optik 201 (2020), 163525, https://doi.org/10.1016/j.ijleo.2019.163525.
[26] Shams A.M. Issa, H.O. Tekin, H.A. Saudi, M.S.I. Koubisy, M. Zhukovsky, Ahmed S. Ali, Hesham, M.H. Zakaly, Fabrication of newly developed Tungsten III-oxide glass family: Physical, Structural, Mechanical, radiation shielding effectiveness, Optik 259 (2022), 169025, https://doi.org/10.1016/j.ijleo.2022.169025.
[27] R. Kurtulus, M.S. Buriahi, Shams A.M. Issa, H.O. Tekin, T. Kavas, E. Kavaz, Physical, structural, mechanical and radiation shielding features of waste pharmaceutical glasses doped with Bi_2O_3, Optik (2022), 169108, https://doi.org/10.1016/j.ijleo.2022.169108.

[28] E. Ilik, G. Kilic, U.G. Issever, S.A. Issa, H.M. Zakaly, H.O. Tekin, Cerium (IV) oxide reinforced Lithium-Borotellurite glasses: a characterization study through physical, optical, structural and radiation shielding properties, Ceram. Int. 48 (1) (2022) 1152–1165, https://doi.org/10.1016/j.ceramint.2021.09.200.
[29] H.O. Tekin, Ghada ALMisned, Shams A.M. Issa, Hesham M.H. Zakaly, A rapid and direct method for half value layer calculations for nuclear safety studies using MCNPX Monte Carlo code, Nucl. Eng. Technol. 54 (2022) 9, https://doi.org/10.1016/j.net.2022.03.037.
[30] E. Ilik, Effect of heavy rare-earth element oxides on physical, optical and gamma-ray protection abilities of zinc-borate glasses, Appl. Phys. A 128 (6) (2022) 1–10, https://doi.org/10.1007/s00339-022-05642-6.
[31] R.U. Erdemir, G. Kilic, D.S. Baykal, G. ALMisned, S.A. Issa, H.M. Zakaly, A. Ene, H.O. Tekin, Diagnostic and therapeutic radioisotopes in nuclear medicine: determination of gamma-ray transmission factors and safety competencies of high-dense and transparent glassy shields, Open Chem. 20 (1) (2022) 517–524, https://doi.org/10.1515/chem-2022-0167.